RSC Advances

ROYAL SOCIETY OF CHEMISTRY

www.rsc.org/advances

Table of Contents Entry

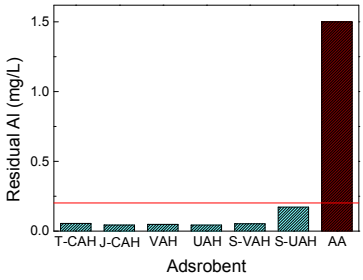

Ultrasonically prepared $Al(OH)_3$ has a high defluoridation capacity and a low residual aluminum concentration in drinking water after defluoridation.

Fluoride Removal from Water Using High-Activity Aluminum Hydroxide Prepared by the Ultrasonic Method

Wei-Zhuo Gai[a,b], Zhen-Yan Deng[a,*] and Ying Shi[b]

[a]*Energy Materials & Physics Group, Department of Physics, Shanghai University, Shanghai 200444, China*

[b]*School of Materials Science and Engineering, Shanghai University, Shanghai 200444, China*

Keywords: Fluoride removal; Aluminum hydroxide; Ultrasonic treatment; Residual aluminum.

*Author to whom correspondence should be addressed. Tel: +86-21-66134334, Fax: +86-21-66134208, E-mail: zydeng@shu.edu.cn

Abstract: Different $Al(OH)_3$ powders were used as the adsorbents for fluoride removal from water. The results showed that the defluoridation performance of ultrasonically prepared $Al(OH)_3$ (UAH) is much better than that of commercial $Al(OH)_3$ and comparable to that of the activated alumina, because the ultrasonic waves effectively break agglomerates in suspension so that the UAH particles are fine and have a beneficial phase constituent. Furthermore, the residual aluminum concentration in aqueous solution after defluoridation by $Al(OH)_3$ was found one order of magnitude lower than that by the activated alumina, below the World Health Organization (WHO) guideline of aluminum (0.2 mg/L) in drinking water. The defluoridation dynamics and mechanism of UAH are discussed in detail.

1. Introduction

Fluoride is an essential mineral for the growth of dental and bones in mammals. Fluoride at a relative low level (0.5-1.5 mg/L) in drinking water is beneficial to human health, which promotes the calcification of dental enamel and maintenance of healthy bones. However, an excessive intake of fluoride for a long period can result in dental fluorosis, skeletal fluorosis, osteoporosis and brittle bones.[1] Therefore, it is necessary to make the fluoride concentration in drinking water maintain at an acceptable level. The WHO has set 1.5 mg/L of fluoride as the upper limit in drinking water.[2]

High fluoride concentration in drinking water comes from two different channels: natural sources and anthropogenic discharge. Fluorides are released into the environment naturally through weathering and dissolution of rock minerals, leading to a high fluoride concentration in groundwater in some areas. On the other hand, the discharge of wastewater with fluorides from various industries, e.g. mining, semiconductor fabricating, electroplating, rubber and fertilizer manufacturing etc., is another cause for fluoride enrichment in groundwater. Most of rural areas and some of urban areas in developing countries use groundwater as the drinking water. As per a conservative estimate, more than 200 million people worldwide are at risk of different forms of "fluorosis" due to excess fluoride in drinking water, especially in Africa, Mexico, China, India, Pakistan, and Thailand.[3]

Fluoride removal from water has long been an engineering challenge, much endeavor has been done to develop effective defluoridation technologies. In order to

reduce fluoride concentration to an acceptable level in drinking water, different methods have been developed such as precipitation, adsorption, ion exchange, membrane separation and electrodialysis, and reverse osmosis.[4,5] Among various defluoridation techniques, adsorption is an environmentally friendly and economically viable method due to its flexibility and simplicity of design, relative ease of operation and low cost.

During the past decades, many natural mineral and biopolymer adsorbents have been used to remove fluoride, e.g. alum sludge, hydroxyapatite, aluminum hydroxide coated rice husk ash, surface modified pumice, modified natural siderite, zeolitic tuff, pseudoboehmite and chitosan shell.[6-13] Although natural mineral and biopolymer adsorbents have a low cost, they have low adsorption capacity and require a complex modification procedure to improve their defluoridation performance. In order to enhance the adsorption capacity of adsorbent, some nanometer metal oxides and hydroxides with high surface area such as nano alumina,[14-16] carbon nanotube supported alumina,[17] manganese-oxide-coated alumina,[18,19] nano boehmite or bayemite,[20-22] double or trimetal hydroxides,[23-27] Fe_3O_4/Al_2O_3, CeO_2/ZrO_2, MnO/Al_2O_3 nanoparticles,[28-30] aluminum sulfate/graphene hydrogel, $MgO/MgCO_3$, and alumina modified graphite,[31-33] etc. have been developed in recent years.

In general, the criteria for selecting an adsorbent mainly include the adsorption capacity, cost, production technology and water quality after fluoride removal. Among various adsorbents, the activated alumina has been commercialized and widely used in many countries due to its high binding affinity with F^- ions and cost-effectiveness.

However, the main disadvantage of activated alumina is its high residual aluminum concentration in aqueous solution after defluoridation. George et al.[34] found that the residual aluminum concentration is up to 1.5 mg/L when the initial fluoride concentration is 10 mg/L and the activated alumina dose is 4 g/L, far beyond the WHO guideline of 0.2 mg/L aluminum in drinking water. A high concentration of aluminum in drinking water could cause Alzheimer's disease.[35] In the aforementioned nanometer adsorbents, few works have the data about the residual aluminum concentration in water after defluoridation. In this work, it was found that a low residual aluminum concentration in drinking water is reached using aluminum hydroxides to remove fluoride, making aluminum hydroxides a promising alternative for the activated alumina.

However, commercial aluminum hydroxides produced by the Bayer process using bauxite has a poor fluoride adsorption capacity.[36] In order to improve the defluoridation performance of aluminum hydroxides, Shimelis et al.[37] prepared aluminum hydroxide adsorbent through hydrolysis of aluminum sulfate. Jia et al.[22] synthesized a feather like bayerite/boehmite adsorbent by a facile one-pot hydrothermal method. However, these methods use alkaline solution and the amount of alkaline solution requires precisely controlling. In a previous work,[38] a high-activity $Al(OH)_3$ was prepared by the reaction of Al with water using an ultrasonic procedure. In this work, the ultrasonically prepared $Al(OH)_3$ was used as the adsorbent for fluoride removal from water, and found that its defluoridation performance is comparable to that of the activated alumina.

2. Experimental procedure

Al powder with an average size of 2.25 μm (99.9% purity, Henan Yuan Yang Aluminum Industry Co., China) and two kinds of commercial $Al(OH)_3$ powders purchased from Tianjin (99.4% purity, Tianjin Damao Chemical Reagent Factory, Tianjin, China, referred to as T-CAH hereafter) and Japan (99.99% purity, 2.5 μm, High Purity Chemical Co., Tokyo, Japan, referred to as J-CAH) were used in the present research. In order to study the defluoridation performance, NaF, NaCl, Na_2SO_4, $NaNO_3$, Na_2HPO_4, NaOH and HCl (analytical reagent grade, Sinopharm Chemical Reagent Co.,Ltd., Shanghai, China) were used in the experiment.

In addition to the commercial $Al(OH)_3$ powders, two other $Al(OH)_3$ suspensions and powders were prepared in this work. One was prepared by reacting pure Al powder with water in a closed glass reactor in vacuum (the initial pressure is 7.4 kPa) at 40°C to form $Al(OH)_3$ suspension (S-VAH), and then filtering by a filter paper and drying at 60°C to form $Al(OH)_3$ powder (VAH).[39] Another was prepared by putting pure Al powder into a beaker with deionized water, then ultrasonically treating in an ultrasonic vessel (40 kHz, 100 W) at 40°C for a time period (~ 2 h) to form $Al(OH)_3$ suspension (S-UAH), and finally filtering by a filter paper and drying at 60°C to form $Al(OH)_3$ powder (UAH).[38]

The fluoride stock solution (1000 mg/L) was prepared by dissolving an appropriate NaF in deionized water. The fluoride solution used for adsorption experiments was prepared by diluting the stock solution to a setting concentration

using deionized water. Adsorption tests were carried out in 250 ml of fluoride solution, and 1 g of $Al(OH)_3$ adsorbent (4 g/L) was used in each test. A magnetic agitation bar with a speed of ~500 rpm was used to stir the mixture of adsorbent and fluoride solution. At a pre-setting time, 10 ml of sample was taken from the adsorption solution and filtrated through a filter with a 0.22 μm polyethersulfone (PES) resin membrane. The residual F^- concentration in filtrate was measured by an ion chromatograph (IC, Model No. MIC-II, Metrohm Co., Switzerland). The F^- removal ratio α can be calculated by the following equation

$$\alpha = \frac{C_0 - C_t}{C_0} \quad (1)$$

where C_0 and C_t are the initial and residual F^- concentration at time t, respectively. Moreover, the residual aluminum concentration in filtrate was measured by an inductively coupled plasma atomic emission spectrometer (ICP-AES, Model No. ICAP 6300, Thermo Fisher Co., USA). All the adsorption tests were conducted three times and the average values were reported.

A zeta potential analyzer (type: ZETASIZER 3000HSA, Malvern Instruments Ltd., UK) was used to measure the zeta (ζ) potential of $Al(OH)_3$ suspension prepared by the ultrasonic procedure (S-UAH). A pH meter (Model No. MP512, Shanghai Sanxin Instrument Co., Shanghai, China) was used to measure the pH value of different solutions. X-ray diffractometry (XRD, Model No. D/max-2200, Rigaku Co., Japan) was used to analyze the phases in different $Al(OH)_3$ powders. Scanning electron microscopy (SEM, Model No. JSM-6700F, JEOL Co., Japan) was used to observe the morphologies of Al and different $Al(OH)_3$ powders.

3. Results and discussion

3.1. Characterization of aluminium hydroxides

Fig. 1 shows the morphologies of as-received pure Al and three kinds of $Al(OH)_3$ powders. It can be seen that Al particles are spherical, their surfaces are dense and smooth (Fig. 1(a)). The surface morphologies of three kinds of $Al(OH)_3$ powders have difference. The particles of J-CAH are large and have a columnar structure (Fig. 1(b)). However, UAH has a flower-like structure and its particles are fine (Fig. 1(d)). VAH also has a flower-like structure, but some of its particles are large and dense. From the morphology analysis, it seems that the surface area of $Al(OH)_3$ powders is in the order of UAH > VAH > J-CAH.

Fig. 2 shows the X-ray diffraction patterns of four kinds of $Al(OH)_3$ powders. It can be seen that T-CAH and J-CAH have a phase of gibbsite and bayerite, respectively. VAH has a phase of bayerite, but UAH has a phase composition of bayerite and boehmite. Furthermore, the diffraction peaks of UAH is wider than those of other $Al(OH)_3$ (see the red arrows), so the grain sizes in UAH are smaller than those in other $Al(OH)_3$, implying that the surface area of UAH is the largest among them, which is consistent with the morphology observation in Fig. 1.

3.2. Fluoride removal performance

Fig. 3(a) shows fluoride removal from aqueous solution with an initial F^- concentration of 20 mg/L using different $Al(OH)_3$ powders or suspensions at 25°C. It can be seen that the preparation methods have a significant impact on the

defluoridation performance of $Al(OH)_3$. The commercial $Al(OH)_3$ powders have a poor F^- adsorption capacity, the final fluoride removal by T-CAH and J-CAH is only 9.5% and 27.3%, respectively. The $Al(OH)_3$ powders and suspensions prepared by the reaction of Al with water in vacuum or using an ultrasonic procedure have a better defluoridation performance than the commercial $Al(OH)_3$ powders. For the $Al(OH)_3$ prepared by the reaction of Al with water, its powders (UAH and VAH) have a quicker defluoridation behavior than its suspensions (S-UAH and S-VAH), but the final fluoride removal by UAH and VAH is lower than that by S-UAH and S-VAH. Among these $Al(OH)_3$ powders and suspensions, UAH has the quickest defluoridation performance and it removes ~75% of fluoride within 5 h, which corresponds to a defluoridation capacity of ~ 3.8 mg/g UAH. This indicates that the defluoridation capacity of UAH is comparable to that of the activated alumina (~2.4 mg/g activated alumina in a similar condition in Ref. 14).

Fig. 3(b) shows fluoride removal from aqueous solution with different initial F^- concentration using UAH at 25°C. It can be seen that the initial F^- concentration has a significant effect on the fluoride removal ratio, which decreases with increasing the initial F^- concentration. When the initial F^- concentration is 10 mg/L, more than 90% of fluoride was removed within 3 h and the residual F^- concentration is ~ 1.0 mg/L, within the guideline value of WHO. This implies that UAH is an effective and viable adsorbent for defluoridation if the F^- concentration in groundwater is below 10 mg/L.

The effect of initial pH value in aqueous solution on the fluoride removal using UAH was investigated, as shown in Fig. 4(a), where the fluoride solution with

different initial pH value was obtained by adding a suitable amount of HCl or NaOH. It can be seen that the final fluoride removal is closely related to the initial pH value. When the initial pH value is between 5 and 9, it almost has no impact on the fluoride removal. When the initial pH value decreases from 5 to 3, the fluoride removal increases. When the initial pH value is > 9, the fluoride removal decreases with increasing the pH value.

In fact, the F^- adsorption onto $Al(OH)_3$ or AOOH is closely related to its surface chemical characteristics, changing pH value will lead to the change in its zeta potential. Fig. 4(b) shows the zeta potential curve of S-UAH, it can be seen that the isoelectric point of S-UAH is at ~ 10.3. When the pH value is below this isoelectric point, the zeta potential of $Al(OH)_3$ suspension is positive, i.e. the $Al(OH)_3$ particles have a positive surface charge.[40] In this case, there is an electrostatic attraction between the $Al(OH)_3$ surfaces and F^- ions, so decreasing pH value from 5 to 3 promotes the F^- adsorption onto UAH. However, when the pH value is above the isoelectric point, the $Al(OH)_3$ particles have a negative surface charge and there is an electrostatic repulsion between the $Al(OH)_3$ surfaces and F^- ions, so increasing pH value inhibits the F^- adsorption when the pH value is > 9 (Fig. 4(a)). Moreover, there is a competition between OH^- and F^- ions for the adsorption sites on $Al(OH)_3$ surfaces at alkaline pH range.[40]

In addition to fluoride, the drinking water often contains other anions such as Cl^-, SO_4^{2-}, NO_3^- and HPO_4^{2-}, etc.,[41] so the co-existing anions in water may influence the defluoridation performance of UAH. Fig. 5(a) shows the fluoride removal from

solution containing 50 mg/L of different co-existing anions separately using UAH at 25°C. It can be seen that Cl^- and NO_3^- ions almost have no effect on the fluoride removal. However, SO_4^{2-} and HPO_4^{2-} ions inhibit the F^- adsorption onto UAH, especially for HPO_4^{2-} ions, which decrease the fluoride removal from ~ 80% to just 24.4%. Fig. 5(b) shows the residual co-existing anions in aqueous solution after defluoridation by UAH. It can be seen that the Cl^- and NO_3^- concentrations have no any change before and after defluoridation, but the concentrations of SO_4^{2-} and HPO_4^{2-} after defluoridation decrease to 47.0 and 4.4 mg/L, respectively. This indicates that SO_4^{2-} and HPO_4^{2-} ions also adsorbed onto UAH surfaces, and there is a competition between F^- and SO_4^{2-}, HPO_4^{2-} ions for the adsorption sites on UAH surfaces.[20]

Fig. 6 shows fluoride removal from solution with different initial F^- concentration using UAH at different temperatures. It can be seen that the defluoridation performance of UAH decreases with increasing the temperature. When the temperature increases from 25°C to 55°C, the fluoride removal decreases from 92.6% to 82.5% and from 68.1% to 45.4% for the initial F^- concentration of 10 and 40 mg/L, respectively, implying that F^- adsorption onto UAH is an exothermic process.[42]

Our adsorption dynamics analyses indicated that the F^- adsorption onto UAH follows the pseudo-second-order adsorption. The adsorption isotherm showed that F^- adsorption onto UAH is a chemical adsorption process. Thermodynamic study confirmed that F^- adsorption onto UAH is an exothermic process, which is favorable and spontaneous in nature (The details are given in the supplementary material).

3.3. Residual aluminum

Aluminum will dissolve into water from adsorbent surface when Al-based adsorbent is used in water treatment. Fig. 7 shows the residual aluminum in aqueous solution after defluoridation by different $Al(OH)_3$ powders or suspensions at 25°C, where the result of activated alumina in a similar condition is added for comparison.[34] Compared with the activated alumina, the residual aluminum concentration in aqueous solution after defluoridation by different $Al(OH)_3$ powders or suspensions is low, which is below the WHO guideline of 0.2 mg/L aluminum in drinking water. Moreover, the residual aluminum concentration in aqueous solution after defluoridation by S-UAH is 0.17 mg/L, which is higher than those by other $Al(OH)_3$ powders. This is because some of the $Al(OH)_3$ particles in S-UAH is probably amorphous, and the solubility of amorphous $Al(OH)_3$ in water is higher than that of crystalline $Al(OH)_3$.[43]

Figs. 8-10 show the effect of pH value, initial F^- concentration and temperature on the residual aluminum concentration in aqueous solution after defluoridation by UAH. When the pH value is between 5.5 and 8.5, the pH value has a small effect on the residual aluminum concentration in aqueous solution, but it is in the range of 0.040-0.055 mg/L (Fig. 8), below the WHO guideline. In fact, the pH value of drinking water is about 6.5-8.5, so UAH is suitable for fluoride removal in drinking water. Fig. 9 indicates that the initial F^- concentration has a significant impact on the residual aluminum concentration and it increases with increasing the F^- concentration. When the initial F^- concentration is > 40 mg/L, the residual aluminum concentration

exceeds the WHO guideline. The possible cause is that at higher initial F^- concentration, $Al(OH)_3$ interacts with F^- ions to form more AlF_x species. As AlF_x has a definite solubility in water, more residual aluminum appears in the solution.[44] Fig. 10 indicates that the residual aluminum concentration increases with increasing the temperature, because the solubility of $Al(OH)_3$ in water increases with the temperature.

3.4. Desorption

An adsorbent is economically effective if the adsorbent can be regenerated and reused. In order to study the desorption capacity of the adsorbent, the used UAH was prepared by filtering the aqueous solution with an initial F^- concentration of 20 mg/L after defluoridation for 24 h at 25°C and then drying the filtered powder. The used UAH was sent to do desorption tests, in each test 0.5 g of the used UAH was added into 100 ml of NaOH solution and then stirred with a magnetic bar at a speed of 500 rpm for 10 h. The desorption capacity of the used UAH can be obtained by measuring the F^- concentration in the desorption solution. Fig. 11 shows the effect of pH value in aqueous solution on the F^- desorption from the used UAH at 25°C. It can be seen that only little F^- ions were released from the used UAH at the pH value < 11. However, the F^- desorption increases abruptly when the pH value is > 11. At pH value of 14, the used UAH released 93.1% of F^- ions within 10 h, indicating that UAH after defluoridation can be regenerated using NaOH solution.[20]

3.5. Physicochemical mechanisms

It is known that there is a layer of hydroxyl groups on $Al(OH)_3$ particle surfaces.

When $Al(OH)_3$ particles are placed in aqueous solution containing F^- ions, the $Al(OH)_3$ particles interact with F^- ions by a surface complexation reaction, which is responsible for the F^- adsorption. To a certain degree, a surface hydroxyl group can be viewed as a Lewis base, which has an oxygen atom as a donor that can coordinate with protons or Al ions. The Al ions are Lewis acid, which can exchange the hydroxyl groups for other coordinating anions.[45] Thus, the specific adsorption of F^- ions onto $Al(OH)_3$ particle surfaces can be described as a ligand exchange, where a hydroxyl group is exchange for a F^- ion. According to the ligand exchange model, such an adsorption is a simple exchange of hydroxyl group for a F^- ion

$$F^- + \equiv AlOH \leftrightarrow \equiv AlF + OH^- \quad (2)$$

where $\equiv AlOH$ is the aluminol group.[46] According to equation (2), the $Al(OH)_3$ will release a OH^- ion after adsorbing a F^- ion, resulting in an increase of pH value.

In order to validate the adsorption mechanism proposed above, Table 1 gives the pH values of the solutions with different F^- concentrations before and after defluoridation by different $Al(OH)_3$ at 25°C. It can be seen that the pH value increases after defluoridation by $Al(OH)_3$. The change (ΔpH) in pH value for UAH is higher than other $Al(OH)_3$ adsorbents, ΔpH increases with increasing the initial F^- concentration and is proportional to the F^- removal amount (Fig. 3). This confirms the above proposed mechanism, because more OH^- ions are released when more F^- ions adsorb onto $Al(OH)_3$ particle surfaces. As the increase in reaction byproduct inhibits the reversible reaction, the F^- removal ratio decreases with increasing F^- concentration (Fig. 3(b)).

From the above analyses, it is clear that F^- ion adsorption onto $Al(OH)_3$ particles is closely related to their surface hydroxyl groups. The surface hydroxyl group density and surface area of $Al(OH)_3$ are two key factors affecting its F^- removal efficiency. In fact, different aluminum oxides and hydroxides have different surface hydroxyl group density. For example, the surface hydroxyl group density of α-Al_2O_3, boehmite and gibbsite is 6, 16.5 and 12 groups per square nanometer, respectively.[46] This may be one reason why T-CAH and J-CAH have different F^- removal performance, because they have different $Al(OH)_3$ phases. Moreover, the good adsorption kinetics of UAH probably also results from its high surface hydroxyl group density, because the UAH has a phase composition of bayerite and boehmite (Fig. 2), and boehmite has a high surface hydroxyl group density as mentioned above.

It is well known that the sonochemical effect of ultrasound in liquid-solid system mainly arises from acoustic cavitation.[47] During cavitation, bubble collapse produces intense heating and high pressure at the interfacial region around cavitation bubbles, which promote the formation of boehmite during the UAH preparation process, because boehmite forms at a higher temperature than bayerite.[48] As aforementioned, the existence of boehmite in UAH is favorable for the F^- removal. In addition, ultrasonic cavitation can create microjets and shock waves, which effectively break agglomerates and increase the $Al(OH)_3$ and AlOOH surface area, leading to a higher F^- removal ratio of UAH than VAH, T-CAH and J-CAH (Fig. 3(a)).

The above analyses indicated that the ultrasonic procedure is an important cause for the high F^- removal of UAH. In order to determine whether the ultrasonic

procedure can improve the F^- removal of J-CAH and VAH, J-CAH and S-VAH were ultrasonically treated for 1 h and then used to do the F^- adsorption tests. Figs. 12 and 13 show the F^- removal from the aqueous solution with an initial F^- concentration of 20 mg/L at 25°C using J-CAH, VAH, S-VAH and those after the ultrasonic treatment. It can be seen that the ultrasonic treatment has a negligible impact on the F^- removal by J-CAH (Fig. 12). However, the ultrasonic treatment greatly improves the F^- removal by VAH and S-VAH (Fig. 13).

In fact, there are many $Al(OH)_3$ soft agglomerates in S-VAH due to its lack of breaking mechanism. After the ultrasonic treatment, the soft agglomerates in S-VAH are broken, which increases the $Al(OH)_3$ surface area, leading to an increase in its F^- removal. However, the agglomerates in J-CAH are hard due to the sintering and grain growth during drying, which have a coalescence between particles and the bonding strength between particles is strong.[39] Therefore, it is not easy to break these hard agglomerates, and the surface area of J-CAH almost has no change after the ultrasonic treatment. This is why the ultrasonic treatment has a negligible impact on the F^- removal by J-CAH.

In fact, the Al-water reaction is a promising hydrogen-generation technology for portable fuel cell application and $Al(OH)_3$ is the byproduct of Al-water reaction.[49-51] Therefore, the Al-water reaction byproduct can be used to remove fluoride in drinking water through the ultrasonic treatment, which provides an ideal and economic way to dispose of the Al-water reaction byproduct.

4. Conclusions

In this work, a high-activity $Al(OH)_3$ powder prepared by the reaction of Al with water using the ultrasonic procedure (UAH) was used as the adsorbent for the fluoride removal from water. It was found that the defluoridation performance of UAH is much better than that of commercial $Al(OH)_3$ powders and comparable to that of the activated alumina. The residual aluminum concentration in aqueous solution after defluoridation by UAH is much lower than that by the activated alumina, making UAH a promising alternative for the activated alumina. The mechanism analyses revealed that the ultrasonic cavitation effectively breaks the agglomerates in $Al(OH)_3$ suspension and promotes the formation of boehmite phase with high surface hydroxyl group density, leading to a high fluoride removal capacity of UAH. The present work provides a new way to dispose of $Al(OH)_3$ produced by the Al-water reaction used for hydrogen generation.

Acknowledgments

We would like to thank the financial supports of the Innovation Program of Shanghai Municipal Education Commission (13ZZ079) and the "085 project" of Shanghai Municipal Education Commission.

References

1 Meenakshi and R. C. Maheshwari, *J. Hazard. Mater.*, 2006, **137**, 456-463.

2 A. Bhatnagar, E. Kumar and M. Sillanpää, *Chem. Eng. J.*, 2011, **171**, 811-840.

3 S. Ayoob, A. K. Gupta and V. T. Bhat, *Crit. Rev. Env. Sci. Tec.*, 2008, **38**, 401-470.

4 M. Mohapatra, S. Anand, B. K. Mishra, D. E. Giles and P. Singh, *J. Environ. Manage.*, 2009, **91**, 67-77.

5 E. Kumar, A. Bhatnagar, W. Hogland, M. Marques and M. Sillanpää, *Chem. Eng. J.*, 2014, **241**, 443-456.

6 M. G. Sujana, R. S. Thakur and S. B. Rao, *J. Colloid Interf. Sci.*, 1998, **206**, 94-101.

7 X. Fan, D. J. Parker and M. D. Smith, *Water Res.*, 2003, **37**, 4929-4937.

8 V. Ganvir and K. Das, *J. Hazard. Mater.*, 2011, **185**, 1287-1294.

9 A. Salifu, B. Petrusevski, K. Ghebremichael, L. Modestus, R. Buamah, C. Aubry and G. L. Amy, *Chem. Eng. J.*, 2013, **228**, 63-74.

10 M. N. Sepehr, V. Sivasankar, M. Zarrabi and M. S. Kumar, *Chem. Eng. J.*, 2013, **228**, 192-204.

11 Y. Shan and H.M. Guo, *Chem. Eng. J.*, 2013, **223**, 183-191.

12 A. Teutli-Sequeira, M. Solache-Ríos, V. Martínez-Miranda and I. Linares-Hernández, *J. Colloid Interf. Sci.*, 2014, **418**, 254-260.

13 Z. Wan, W. Chen, C. Liu, Y. Liu and C. L. Dong, *J. Colloid Interf. Sci.*, 2015, **443**, 115-124.

14 S. Ghorai and K. K. Pant, *Chem. Eng. J.*, 2004, **98**, 165-173.

15 L. M. Camacho, A. Torres, D. Saha and S. G. Deng, *J. Colloid Interf. Sci.*, 2010, **349**, 307-313.

16 E. Kumar, A. Bhatnagar, U. Kumar and M. Sillanpää, *J. Hazard. Mater.*, 2011, **186**, 1042-1049.

17 Y. H. Li, S. Wang, X. Zhang, J. Wei, C. Xu, Z. Luan, D. Wu and B. Wei, *Environ. Technol.*, 2003, **24**, 391-398.

18 S. M. Maliyekkal, A. K. Sharma and L. Philip, *Water Res.*, 2006, **40**, 3497-3506.

19 S. X. Teng, S. G. Wang, W. X. Gong, X. W. Liu and B. Y. Gao, *J. Hazard. Mater.*, 2009, **168**, 1004-1011.

20 S. G. Wang, Y. Ma, Y. J. Shi and W. X. Gong, *J. Chem. Technol. Biotechnol.*, 2009, **84**, 1043-1050.

21 R. P. Liu, W. X. Gong, H. C. Lan, Y. P. Gao, H. J. Liu and J. H. Qu, *Chem. Eng. J.*, 2011, **175**, 144-149.

22 Y. Jia, B. S. Zhu, Z. Jin, B. Sun, T. Luo, X. Y. Yu, L. T. Kong and J. H. Liu, *J. Colloid Interf. Sci.*, 2015, **440**, 60-67.

23 J. B. Zhou, Y. Cheng, J. G. Yu and G. Liu, *J. Mater. Chem.*, 2011, **21**, 19353-19361.

24 Q. Chang, L. H. Zhu, Z. H. Luo, M. Lei, S. C. Zhang and H. Q. Tang, *Ultrason. Sonochem.*, 2011, **18**, 553-561.

25 B. Zhao, Y. Zhang, X. M. Dou, X. M. Wu and M. Yang, *Chem. Eng. J.*, 2012, **185-186**, 211-218.

26 X. M. Wu, Y. Zhang, X. M. Dou, B. Zhao and M. Yang, *Chem. Eng. J.*, 2013, **223**, 364-370.

27 T. Zhang, Q. R. Li, H. Y. Xiao, Z. Y. Mei, H. X. Lu and Y. M. Zhou, *Appl. Clay*

Sci., 2013, **72**, 117-123.

28 L. Y. Chai, Y. Y. Wang, N. Zhao, W. C. Yang and X. Y. You, *Water Res.*, 2013, **47**, 4040-4049.

29 J. Wang, W. H. Xu, L. Chen, Y. Jia, L. Wang, X. J. Huang and J. H. Liu, *Chem. Eng. J.*, 2013, **231**, 198-205.

30 S. Alemu, E. Mulugeta, F. Zewge and B. S.Chandravanshi, *Environ. Technol.,* 2014, **35**, 1893-1903.

31 Y. Q. Chen, Q. K. Zhang, L. B. Chen, H. Bai and L. Li, *J. Mater. Chem. A*, 2013, **1**, 13101-13110.

32 K. S. Zhang, S. B. Wu, X. L. Wang, J. Y. He, B. Sun, Y. Jia, T. Luo, F. L. Meng, Z. Jin, D. Y. Lin, W. Shen, L. T. Kong and J. H. Liu, *J. Colloid Interf. Sci.*, 2015, **446**, 194-202.

33 H. Y. Jin, Z. J. Ji, J. Yuan, J. Li, M. Liu, C. H. Xu, J. Dong, P. Hou and S. Hou, *J. Alloy. Compd.*, 2015, **620**, 361-367.

34 S. George, P. Pandit and A. B. Gupta, *Water Res.*, 2010, **44**, 3055-3064.

35 V. Rondeau, D. Commenges, H. Jacqmin-Gadda and J. F. Dartigues, *Am. J. Epidemiol.*, 2000, **152**, 59-66.

36 F. Habashi, *Hydrometallurgy*, 2005, **79**, 15-22.

37 B. Shimelis, F. Zewge and B. S. Chandravanshi, *Bull. Chem. Soc. Ethiop.*, 2006, **20**, 17-34.

38 Y. Yang, W. Z. Gai, Z. Y. Deng and J. G. Zhou, *Int. J. Hydrogen Energy*, 2014, **39**, 18734-18742.

39 W. Z. Gai and Z. Y. Deng, *Int. J. Hydrogen Energy*, 2014, **39**, 13491-13497.

40 Y. Ku and H. M. Chiou, *Water Air Soil Poll.*, 2002, **133**, 349-360.

41 W. Z. Gai and Z. Y. Deng, *J. Power. Sources*, 2014, **245**, 721-729.

42 M. G. Sujana, G. Soma, N. Vasumathi and S. Anand, *J. Fluorine Chem.*, 2009, **130**, 749-754.

43 J. L. R. Bahena, A. R. Cabrera, A. L. Valdivieso and R. H. Urbina, *Sep. Sci. Technol.*, 2002, **37**, 1973-1987.

44 H. Farrah, J. Slavek and W. F. Pickering, *Aust. J. Soil Res.*, 1987, **25**, 55-69.

45 R. Kummert and W. Stumm, *J. Colloid Interf. Sci.*, 1980, **75**, 373-385.

46 G. Sposito, *Environmental chemistry of aluminum*, CRS Press, 1996.

47 K. S. Suslick and G. J. Price, *Annu. Rev. Mater. Sci.*, 1999, **29**, 295-326.

48 W. Z. Gai, W. H. Liu, Z. Y. Deng and J. G. Zhou, *Int. J. Hydrogen Energy*, 2012, **37**, 13132-13140.

49 Z. Y. Deng, J. M. F. Ferreira, Y. Tanaka and J. H. Ye, *J. Am. Ceram. Soc.*, 2007, **90**, 1521-1526.

50 Z. Y. Deng, J. M. F. Ferreira and Y. Sakka, *J. Am. Ceram. Soc.*, 2008, **91**, 3825-3934.

51 C. S. Fang, W. Z. Gai and Z. Y. Deng, *J. Am. Ceram. Soc.*, 2014, **97**, 44-47.

Figure captions

Fig. 1 SEM micrographs of pure Al powder with an average particle size of 2.25 μm

(a), commercial $Al(OH)_3$ powder purchased from Japan (J-CAH) (b), $Al(OH)_3$ powders prepared by the reaction of 2.25 μm Al powder with water in vacuum (VAH) (c) and using an ultrasonic procedure (UAH) (d), respectively.

Fig. 2 X-ray diffraction patterns of different $Al(OH)_3$ powders: (a) T-CAH, (b) J-CAH, (c) VAH and (d) UAH.

Fig. 3 Fluoride removal from aqueous solution at 25°C (a) with an initial F^- concentration of 20 mg/L using different $Al(OH)_3$ powders or suspensions and (b) with different initial F^- concentrations using UAH.

Fig. 4 (a) Effect of pH value on fluoride removal from aqueous solution using UAH at 25°C (initial F^- concentration = 20 mg/L, contact time = 24 h) and (b) Zeta potential curve for S-UAH.

Fig. 5 (a) Effect of co-existing anions on fluoride removal from aqueous solution using UAH at 25°C and (b) residual co-existing anions in aqueous solution after defluoridation (initial co-existing anion concentration = 50 mg/L, initial F^- concentration = 20 mg/L, contact time = 24 h).

Fig. 6 Effect of temperature on fluoride removal from aqueous solution using UAH, where the initial F^- concentrations in (a) and (b) are 10 and 40 mg/L, respectively.

Fig. 7 Residual Al in aqueous solution at 25°C after defluoridation using different adsorbents (initial F^- concentration = 20 mg/L, contact time = 24 h). The result of activated alumina (AA) is added for comparison[34] and the red line represents the WHO guideline of aluminum in drinking water.

Fig. 8 Residual Al in aqueous solution with different initial pH values at 25°C after

defluoridation using UAH (initial F^- concentration = 20 mg/L, contact time = 24 h).

Fig. 9 Residual Al in aqueous solution with different initial F^- concentration at 35°C after defluoridation using UAH (contact time = 24 h).

Fig. 10 Residual Al in aqueous solution at different temperatures after defluoridation using UAH (initial F^- concentration = 10 mg/L, contact time = 24 h).

Fig. 11 Effect of pH value in aqueous solution on desorption of F^- ions from the used UAH at 25 °C, where the desorption time is 10 h and the used UAH adsorbed fluoride in an aqueous solution with an initial F^- concentration of 20 mg/L at 25 °C for 24 h.

Fig. 12 Fluoride removal from aqueous solution with an initial F^- concentration of 20 mg/L at 25°C using commercial $Al(OH)_3$ powder (J-CAH) and those after the ultrasonic treatment, where "S-J-CAH, US 1h" is the $Al(OH)_3$ suspension prepared by adding J-CAH into deionized water and then ultrasonically treating for 1 h, and "J-CAH, US 1h" is the $Al(OH)_3$ powder obtained through filtering and drying the "S-J-CAH, US 1h". For comparison, the defluoridation curves of S-UAH and UAH are added.

Fig. 13 Fluoride removal from aqueous solution with an initial F^- concentration of 20 mg/L at 25°C using (a) S-VAH and (b) VAH and those after ultrasonic treatment, where "S-VAH, US 1h" is the $Al(OH)_3$ suspension prepared by ultrasonically treating S-VAH for 1 h and "VAH, US 1h" is the $Al(OH)_3$ powder obtained by filtering and drying the "S-VAH, US 1h". For comparison, the defluoridation curves of S-UAH and UAH are added.

Table 1 pH values of the solution before and after defluoridation using different adsorbents at 25°C.

Adsorbent	pH (before defluoridation)	pH (after defluoridation)	ΔpH
T-CAH, 20 mg/L	7.18	7.36	0.18
J-CAH, 20 mg/L	7.22	7.51	0.29
S-VAH, 20 mg/L	7.37	7.76	0.39
S-UAH, 20 mg/L	7.53	8.27	0.74
VAH, 20 mg/L	7.38	7.62	0.24
UAH, 10 mg/L	6.82	6.98	0.16
UAH, 20 mg/L	7.03	7.51	0.48
UAH, 30 mg/L	7.35	8.05	0.70
UAH, 40 mg/L	7.46	8.53	1.07

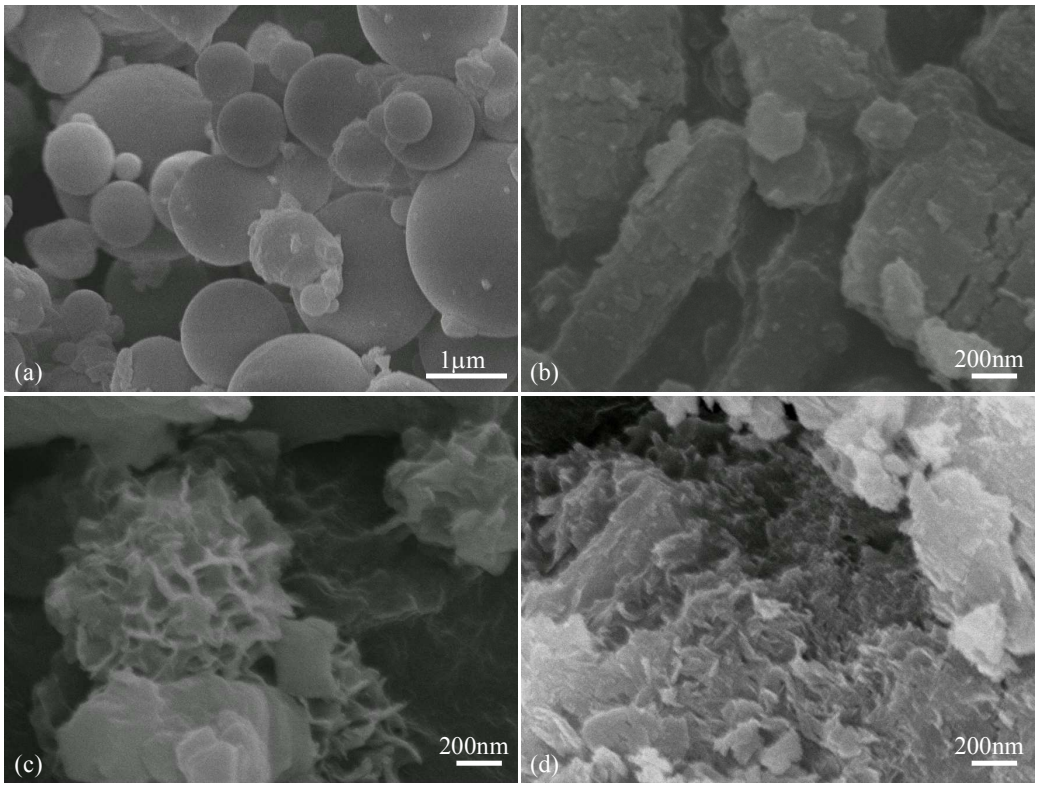

Fig. 1 SEM micrographs of pure Al powder with an average particle size of 2.25 μm (a), commercial $Al(OH)_3$ powder purchased from Japan (J-CAH) (b), $Al(OH)_3$ powders prepared by the reaction of 2.25 μm Al powder with water in vacuum (VAH) (c) and using an ultrasonic procedure (UAH) (d), respectively.

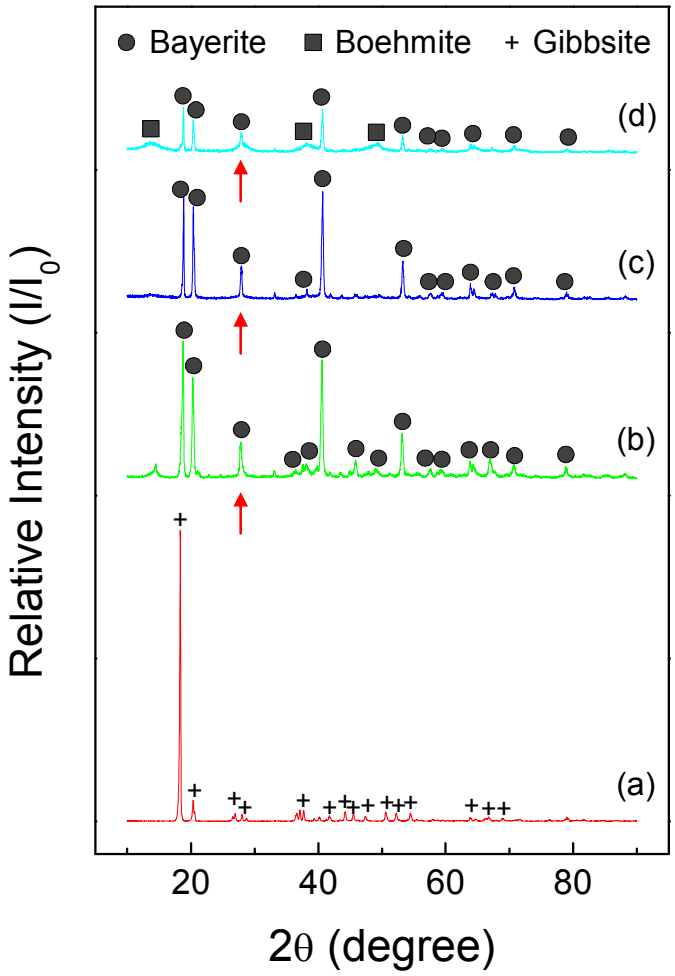

Fig. 2 X-ray diffraction patterns of different $Al(OH)_3$ powders: (a) T-CAH, (b) J-CAH, (c) VAH and (d) UAH.

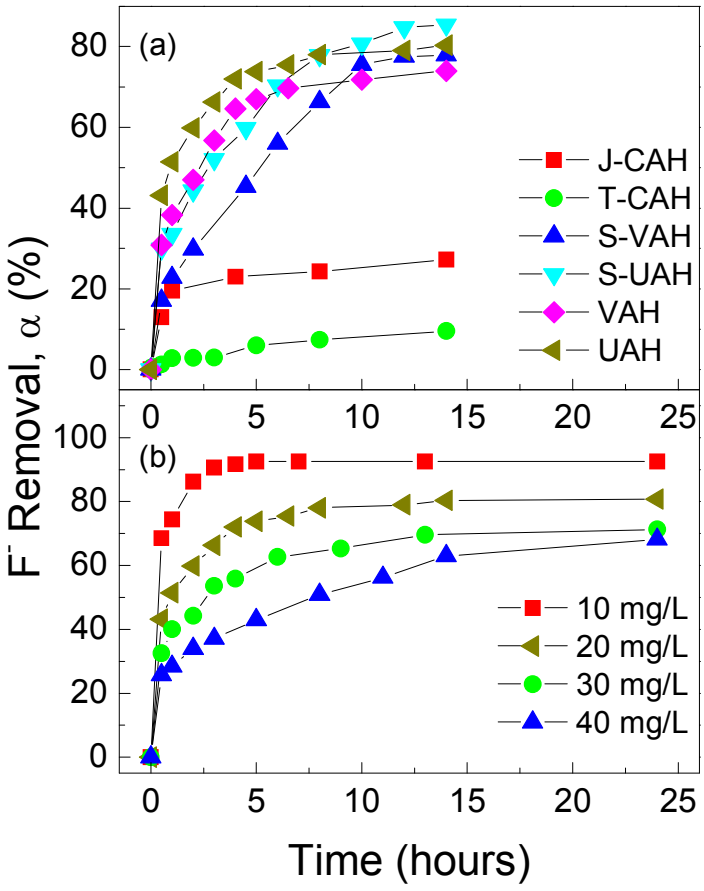

Fig. 3 Fluoride removal from aqueous solution at 25°C (a) with an initial F^- concentration of 20 mg/L using different $Al(OH)_3$ powders or suspensions and (b) with different initial F^- concentrations using UAH.

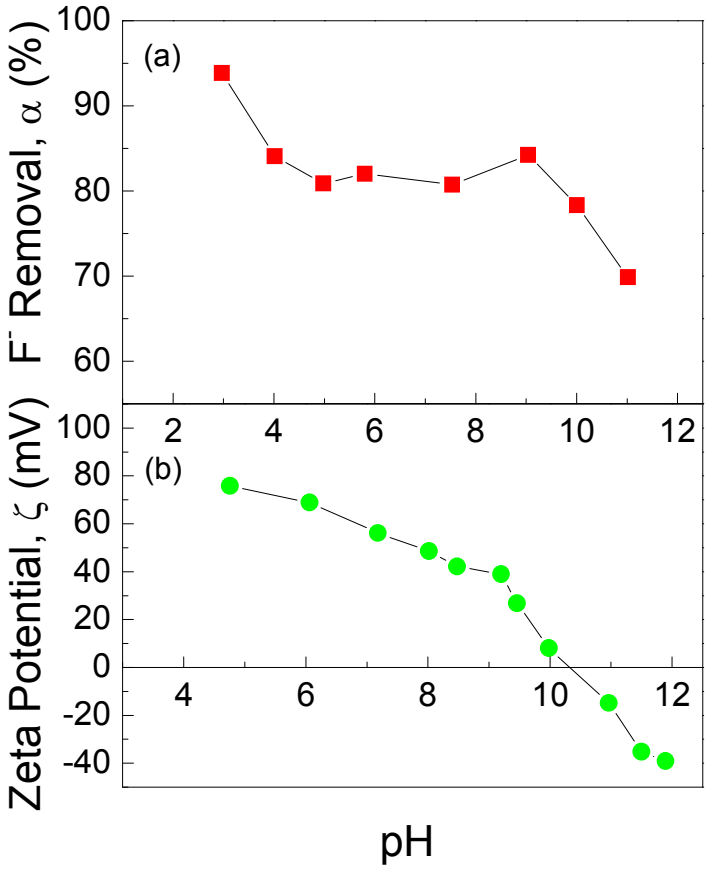

Fig. 4 (a) Effect of pH value on fluoride removal from aqueous solution using UAH at 25°C (initial F^- concentration = 20 mg/L, contact time = 24 h) and (b) Zeta potential curve for S-UAH.

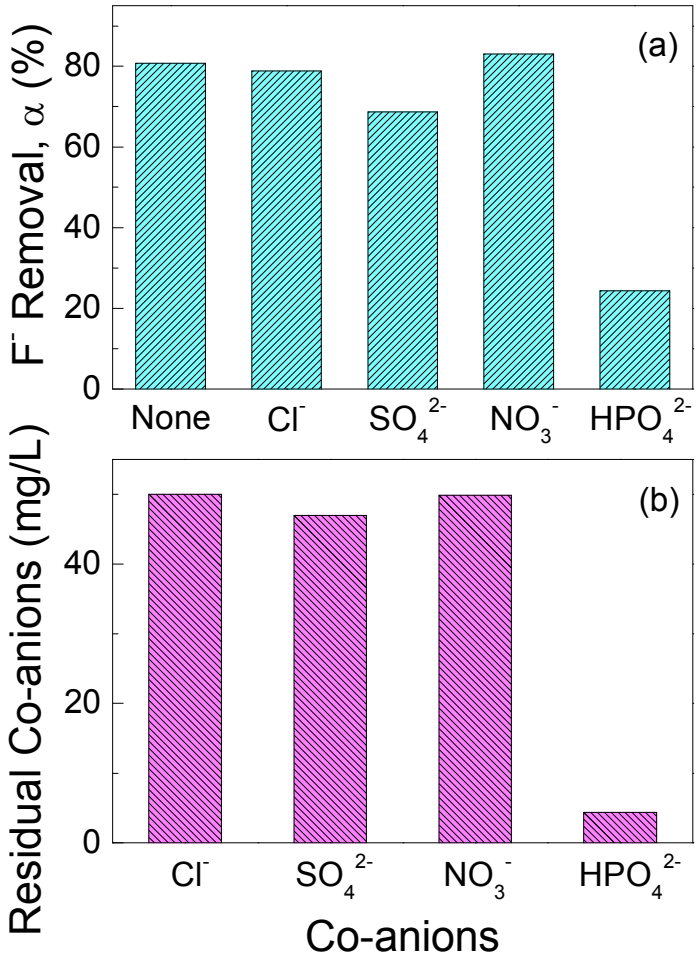

Fig. 5 (a) Effect of co-existing anions on fluoride removal from aqueous solution using UAH at 25°C and (b) residual co-existing anions in aqueous solution after defluoridation (initial co-existing anion concentration = 50 mg/L, initial F^- concentration = 20 mg/L, contact time = 24 h).

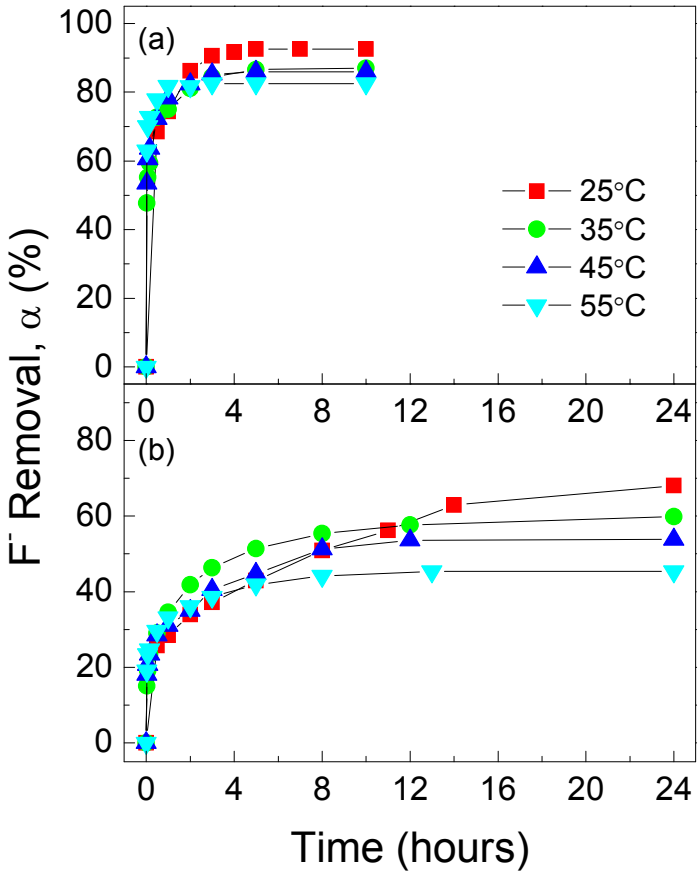

Fig. 6 Effect of temperature on fluoride removal from aqueous solution using UAH, where the initial F^- concentrations in (a) and (b) are 10 and 40 mg/L, respectively.

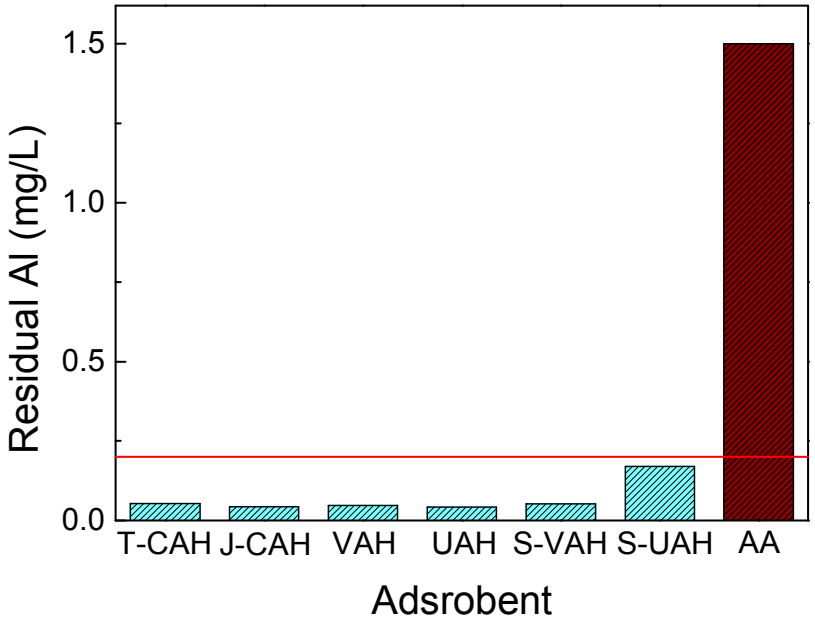

Fig. 7 Residual Al in aqueous solution at 25°C after defluoridation using different adsorbents (initial F^- concentration = 20 mg/L, contact time = 24 h). The result of activated alumina (AA) is added for comparison[34] and the red line represents the WHO guideline of aluminum in drinking water.

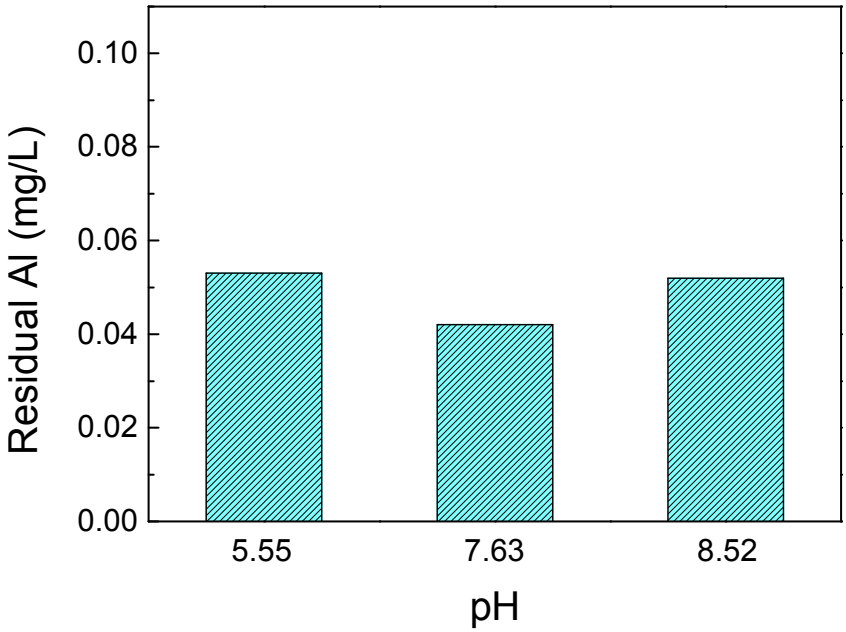

Fig. 8 Residual Al in aqueous solution with different initial pH values at 25°C after defluoridation using UAH (initial F^- concentration = 20 mg/L, contact time = 24 h).

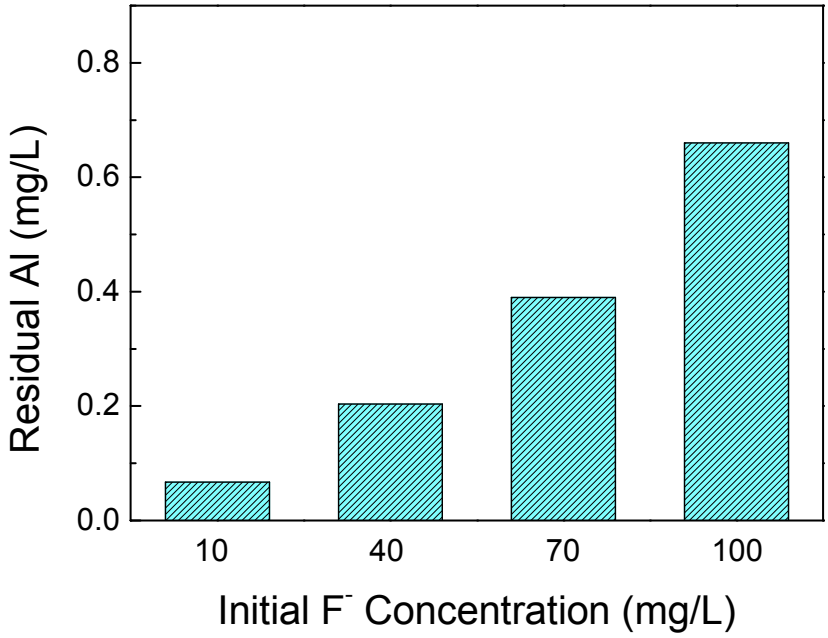

Fig. 9 Residual Al in aqueous solution with different initial F^- concentration at 35°C after defluoridation using UAH (contact time = 24 h).

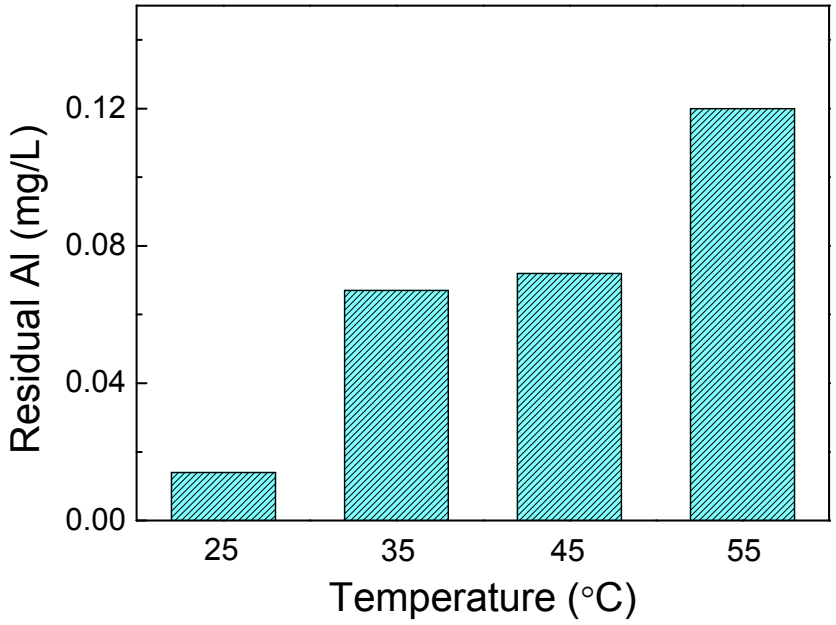

Fig. 10 Residual Al in aqueous solution at different temperatures after defluoridation using UAH (initial F^- concentration = 10 mg/L, contact time = 24 h).

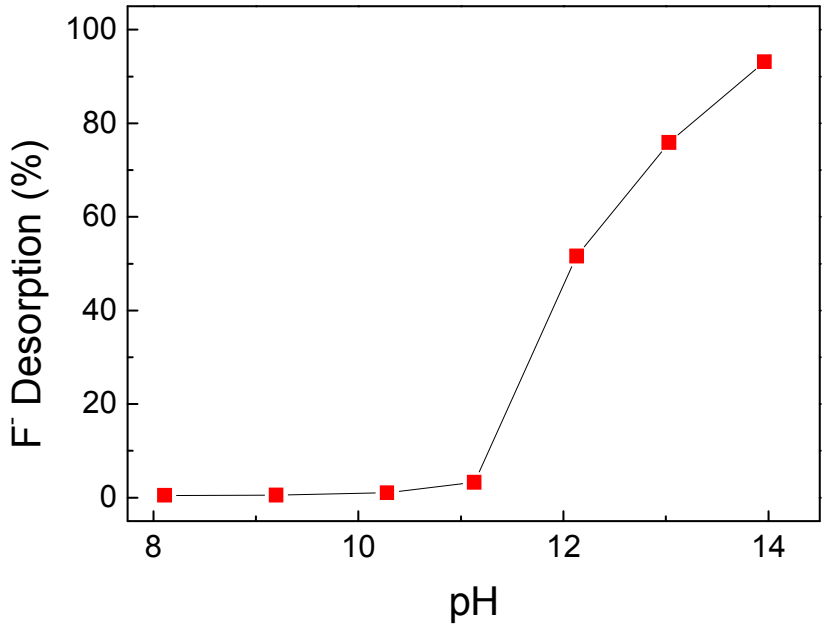

Fig. 11 Effect of pH value in aqueous solution on desorption of F^- ions from the used UAH at 25 °C, where the desorption time is 10 h and the used UAH adsorbed fluoride in an aqueous solution with an initial F^- concentration of 20 mg/L at 25 °C for 24 h.

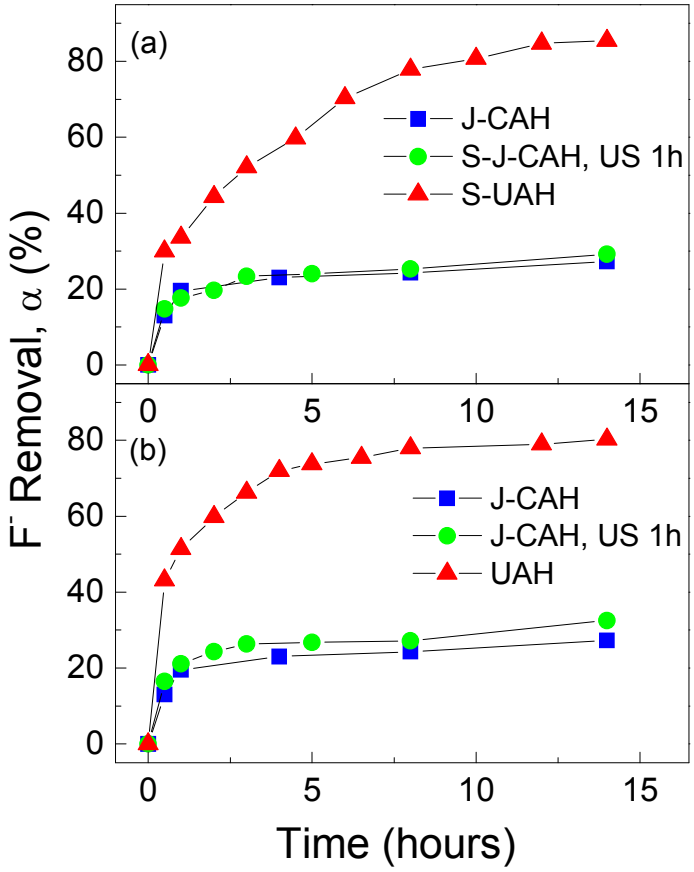

Fig. 12 Fluoride removal from aqueous solution with an initial F^- concentration of 20 mg/L at 25°C using commercial $Al(OH)_3$ powder (J-CAH) and those after the ultrasonic treatment, where "S-J-CAH, US 1h" is the $Al(OH)_3$ suspension prepared by adding J-CAH into deionized water and then ultrasonically treating for 1 h, and "J-CAH, US 1h" is the $Al(OH)_3$ powder obtained through filtering and drying the "S-J-CAH, US 1h". For comparison, the defluoridation curves of S-UAH and UAH are added.

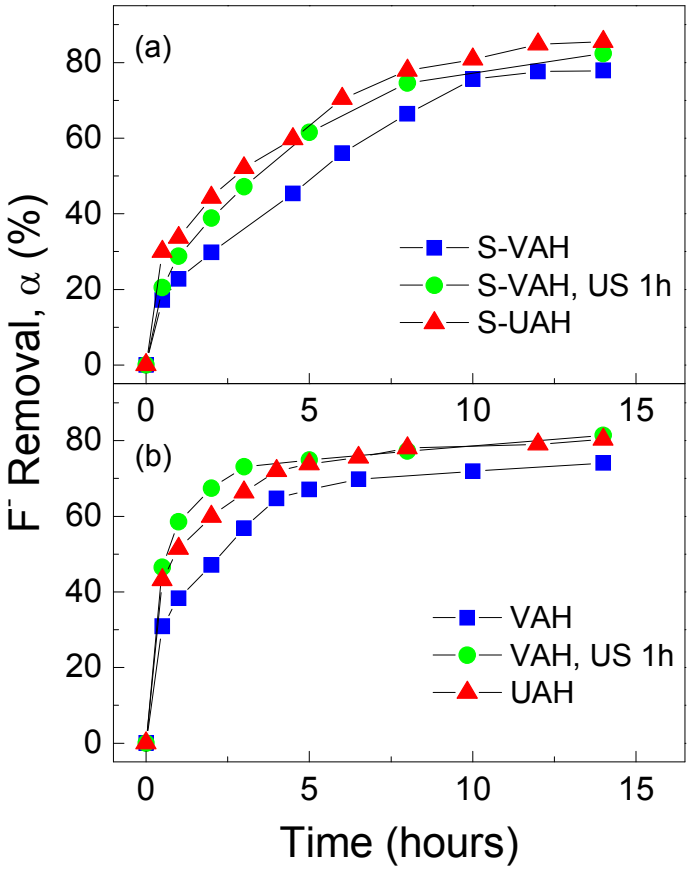

Fig. 13 Fluoride removal from aqueous solution with an initial F^- concentration of 20 mg/L at 25°C using (a) S-VAH and (b) VAH and those after ultrasonic treatment, where "S-VAH, US 1h" is the $Al(OH)_3$ suspension prepared by ultrasonically treating S-VAH for 1 h and "VAH, US 1h" is the $Al(OH)_3$ powder obtained by filtering and drying the "S-VAH, US 1h". For comparison, the defluoridation curves of S-UAH and UAH are added.